

Floquet and Anomalous Floquet Weyl Semimetals

Yufei Zhu,¹ Tao Qin,² Xinxin Yang,¹ Gao Xianlong,^{1,*} Zhaoxin Liang^{1,†}

¹*Department of Physics, Zhejiang Normal University, Jinhua 321004, China*

²*Department of Physics, School of Physics and Materials Science, Anhui University, Hefei, Anhui Province 230601, China*

(Dated: June 19, 2022)

The periodic driving of a quantum system can enable new topological phases without analogs in static systems. This provides a route towards preparing non-equilibrium quantum phases rooted into the non-equilibrium nature by periodic driving engineering. Motivated by the ongoing considerable interest in topological semimetals, we are interested in the novel topological phases in the periodically driven topological semimetals without a static counterpart. We propose to design non-equilibrium topological semimetals in the regime of weakly driving field where the spectrum width of shares the same magnitude with the driving frequency. We identify two novel types of non-equilibrium Weyl semimetals (i.e., Floquet and anomalous Floquet Weyl semimetals) that do not exhibit analogues in equilibrium. The proposed setup is shown to be experimentally feasible using the state-of-the-art techniques used to control ultracold atoms in optical lattices.

At the heart of modern physics are the discovery and control of new phases of matter, highlighted by the foundational aspects of our understanding of periodic driving, which provides wholly new types of topological phases without analogues in equilibrium [1–15]. A paradigmatic example is given by the periodically-driven two-dimensional Dirac model [2, 4, 5, 16–19], where robust chiral edge states can appear even though the Chern numbers of all bulk Floquet bands are zero. A system exhibiting this anomalous behavior has been recently realized using microwave photonic networks [20]. Heretofore, such investigations of periodically driving a quantum system are largely restricted to static system that are topological insulators. Meanwhile, considerable efforts have been devoted to investigate various intriguing phenomena associated with Weyl points such as the Fermi arc surface states [21–24] and chiral anomaly [25–32]. Unlike topological insulators, whose gapless excitations are always at the sample boundary, topological semimetals host gapless fermions in the bulk. An outstanding challenge is to realize novel non-equilibrium topological phases in periodically-driven topological semimetals without analogs in static systems. Another challenge is to extend the periodic driving from an insulator to semimetals with the emphasis on capturing the gapless nature of the energy spectra of the static counterpart [33, 34]. These considerations motivate the search for the novel scenarios of periodically-driven topological Weyl semimetals.

In this Letter, we uncover and analyze two novel types of non-equilibrium Weyl semimetals, i.e., Floquet and anomalous Floquet Weyl semimetals, which do not exhibit analogues in equilibrium. The former is referred to as the case of periodically-driven systems, which are designed to be Floquet Weyl semimetals with the nontrivial topological phases, although the equilibrium counterpart is topologically trivial. In the latter case, we demonstrate the topological appearance in the stroboscopic dynamics

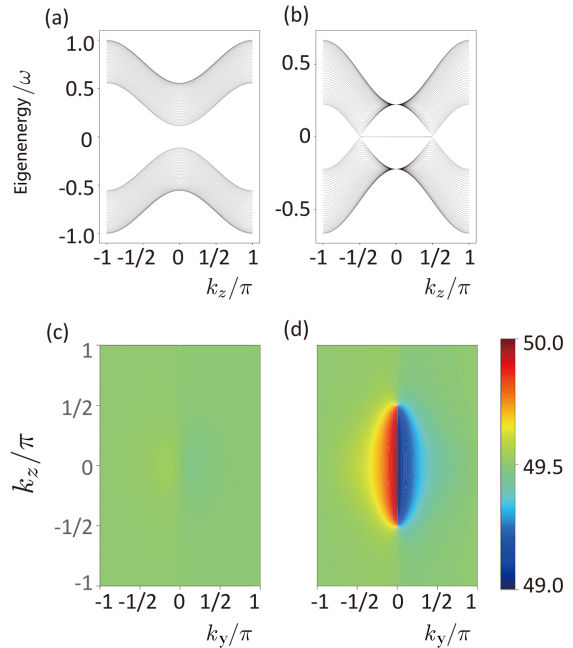


FIG. 1. Energy spectrum of the static Hamiltonian $H_0(k_x = 0, y, k_z)$ in cylindrical geometry with edges along the y -direction and periodic in x - and z -directions; $t_0 = t_s = 1.0$. We choose t_0 as the energy unit. The spectrum for $m = 4.0t_0 < m_c$ in (b) shows that $k_z = \pm \frac{\pi}{2}$ is the z component for the position of Weyl points, while there are no Weyl points for $m = 7.0t_0 > m_c$ in (a). Correspondingly, the position of the hybrid Wannier center, directly related to the Chern number, is shown in (c) and (d) with lattice being periodic in y and z directions and finite in the x direction. There is a shift in one lattice site if k_z is between $k_c = \pm \frac{\pi}{2}$ with $m = 7.0t_0$ in (d), with a shift smaller than one for $m = 4.0t_0$ in (d).

of a periodically driven system. Note that our work is different from Ref. [35], the authors of which were interested

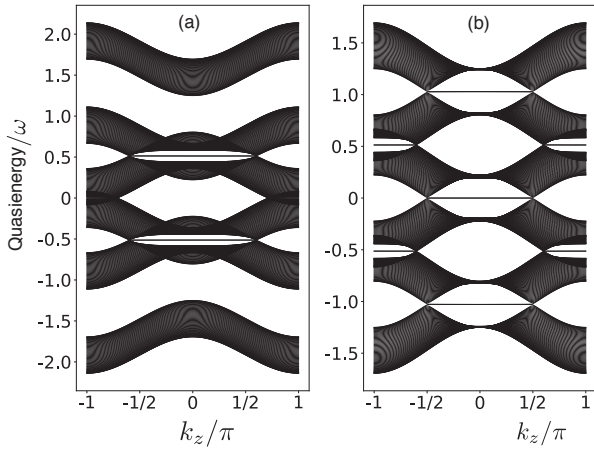


FIG. 2. Truncated Floquet Hamiltonian spectrum with the layer $k_x = 0$ in the cylindrical geometry of k_z good quantum number and y direction open boundary. The horizontal axis denotes the crystal momentum k_z , and the vertical one denotes quasi-energy in the units of driving frequency ω . The parameters are chosen as $\Delta = 1.5$, $t_0 = t_s = 1.0$, $m = 7.0t_0$ (a) and $m = 4.0t_0$ (b). According to the static topologically trivial case, the top and bottom bands should contribute zero Chern numbers. However, we localized edge modes that connected two Weyl points in different m -index bands

in a circularly polarized light driving nodal line semimetals into Weyl semimetals. However, the emphasis and value of this work is on realizing non-equilibrium Weyl semimetals in the intermediate-frequency limit without the analogues in equilibrium. Therefore, our approach goes conceptually beyond high-frequency driving models in that we consider the full quasi-energy spectrum without involving adiabatic projections.

Floquet and Anomalous Floquet Weyl Semimetals—As the paradigmatic example of the two-band Hamiltonian on a square lattice hosting the topological Weyl semimetals [36] (WSM), we consider its time-dependent lattice version:

$$H(\mathbf{k}) = \mathbf{d}(\mathbf{k}) \cdot \boldsymbol{\sigma} + \Delta_0 \sigma_z \cos \omega t, \quad (1)$$

where $\mathbf{d} = (2t_s \sin k_x, 2t_s \sin k_y, m - 2t_0(\cos k_x + \cos k_y + \cos k_z))$ and $\boldsymbol{\sigma} = (\sigma_x, \sigma_y, \sigma_z)$ are the 2×2 Pauli matrices. The t_s and t_0 of Hamiltonian (1) denote the hopping amplitudes of spin-flipping hopping in the x - y plane and spin-preserving hopping along all three dimensions and m represents the Zeeman field for tuning WSM states. The last term in Hamiltonian (1) denotes the periodically-driven term.

Without the periodically-driven term, i.e., $\Delta_0 = 0$ in Hamiltonian (1), two Weyl points (WPs) exist, which are located at the points of $(0, 0, \pm \arccos((m - 4t_0)/2t_0))$ for $2t_0 < m < 6t_0$. To characterize the topological properties of WSM, treating k_z as an effective parameter and reducing the original 3D system to k_z -dependent effective 2D subsystems is necessary. For a given $k_z \neq k_c$, the

bulk bands are fully gapped, and the slice Chern number can be well defined with $\mathbf{n} = (d_x, d_y, d_z)/|\mathbf{d}(\mathbf{k})|$ as $C(k_z) = 1/(4\pi) \int d^2\mathbf{k} \mathbf{n} \cdot \partial_{k_x} \mathbf{n} \times \partial_{k_y} \mathbf{n} = 1$ for $2t_0 < m < 6t_0$ [see Figs. 1 (b) and (d)] while $C(k_z) = 0$ [see Figs. 1 (a) and (c)]. The hybrid Wannier center is defined as $\langle n_x(k_y, k_z) \rangle = \sum_{i_x} i_x \rho(i_x, k_y, k_z) / \sum_{i_x} \rho(i_x, k_y, k_z)$ where i_x is the index for lattice sites and $\rho(i_x, k_y, k_z)$ is the occupied density of states. The Chern number is related to the hybrid Wannier center by $C = \delta \langle n_x(k_y, k_z) \rangle$. Therefore, WSM appears as a transitional state between a trivial insulator and a topological insulator as shown in Fig. 1 (d).

With periodic driving [i.e., $\Delta_0 \neq 0$ in Hamiltonian (1)] the dynamics of the model system are governed by the time-periodic Hamiltonian of $H(t+T) = H(t)$. Our goal is to find the unique topological characteristics of periodically-driven systems without analogs in equilibrium.

To illustrate the analogies and differences from the static counterpart, and in particular to motivate the construction of unique topological characteristics without the analogies of the static system, our strategy is to obtain the effective Hamiltonian of our model system within the rotating wave approximation by making the unitary transformation $U(\mathbf{k}, t) = P_+ + P_- e^{i\omega t}$. Here, P_+ and P_- are the projectors on the upper and lower bands of Hamiltonian (1) with $\Delta_0 = 0$. Thus, the effective Hamiltonian is

$$H_{\text{eff}} = \left(|\mathbf{d}| - \frac{\omega}{2} - \frac{1}{2} \Delta_0 \hat{d}_z \right) \mathbf{d} \cdot \boldsymbol{\sigma} + \frac{1}{2} \Delta_0 \sigma_z. \quad (2)$$

Specifically, Hamiltonian (2) can be simplified as $H_{\text{eff}} = (m - \omega/2) - 2t_0(2 + \cos k_z)\sigma_z$ when $k_x = k_y = 0$. It is clear that with respect to Hamiltonian (1), the key physics underlying Hamiltonian (2) is the renormalization of the effective parameter of $m_{\text{eff}} = m - \omega/2$, which induces the unique non-equilibrium topological phenomena [e.g., $2t_0 < m_{\text{eff}} < 6t_0$, see Figs. 2 (a)] from otherwise trivial static systems (e.g. $m > 6t_0$). We noticed that similar version of Floquet topological Weyl semimetals is given by Floquet topological insulators in Ref. [4].

We are interested in the emergence of Floquet Weyl semimetals as counterparts of Floquet topological insulators [4]. Starting with the topologically trivial phase ($m = 8$), we study the effects of the periodic modulation of Hamiltonian (1) (the last term), which is supposed to create transitions between the valence and conduction band at resonance and this typically opens gaps at the crossing points. The resulting bands exhibit non-zero Chern numbers, which correspond to Floquet Weyl semimetals, as shown in Fig. 2 (a).

The abovementioned intuitive understanding of the emergent Floquet Weyl semimetal is limited to the analytical results of the high-frequency limit, i.e. the driving frequency ω is much larger than the other energy scale of the model system. In the most general case, the exact

time evolution operator of Hamiltonian can be computed as

$$U(\mathbf{k}, t) = \mathcal{T} \exp \left\{ -i \int_0^t H(\mathbf{k}, t') dt' \right\}, \quad (3)$$

where \mathcal{T} is the time-ordering operator. Notice that U is periodic in k_x , k_y and t . Motivated by Ref. [5], we can use U to characterize the non-equilibrium topological properties of time-dependent Hamiltonian (1) by defining a slice winding number

$$W_F(k_z) = \frac{1}{8\pi^2} \int dt d\mathbf{k} \text{Tr} (U^{-1} \partial_t U [U^{-1} \partial_{k_x} U, U^{-1} \partial_{k_y} U]). \quad (4)$$

On the basis of Eq. (4), we emphasize that the underlying physical mechanism is that the micromotion that takes place within each driving period is crucial for the topological classification of periodically driven systems, which differs from the Chern number invariant in non-driven systems, which depend only on projectors onto the band of Floquet states.

Novel types of non-equilibrium phases may emerge owing to the difference between the winding number and the Chern numbers of Floquet bands. By examining the gap centered at quasi-energy $-\pi/T$, as shown in Fig. 2 (b), we expect to determine chiral edge modes spanning this gap on the basis of the effective Hamiltonian (2). The further analytical calculation to the lowest order in Δ_0 shows that the Chern number at quasi-energy $-\pi/T$ is equal to zero. However, WPs between the band of $l = 0$ and $l = -1$ exist. We refer to this type of non-equilibrium Weyl semimetals as anomalous Floquet Weyl semimetals, where the topology can only be explained by the winding number of Eq. (4).

Numerical results— Above, we developed the intuitive physical pictures of Floquet Weyl semimetals and anomalous Floquet Weyl Semimetals. Below, we justify the existence of Floquet Weyl semimetals and anomalous Floquet Weyl Semimetals by solving Hamiltonian (1) with exact numerical methods.

The general Floquet states corresponding to Hamiltonian (1) obey $[H(t) - i\partial_t]|\psi_n(t)\rangle = E_n|\psi_n(t)\rangle$ with $|\psi_n(t)\rangle = |\psi_n(t+T)\rangle$ and generate the quasi-energy E_n (hereafter $\hbar = 1$). We evolve Floquet states at any initial time $t = 0$ by time-evolution operator over one period. Thus, $U(T)|\psi_n(0)\rangle = e^{-iE_n T}|\psi_n(0)\rangle$ becomes an eigenvalue equation, where $e^{-iE_n T}$ is invariant under $E_n + l\omega$ ($l \in \mathbb{N}$). Hence, the quasi-energy E_n possesses periodicity, and $U(T) = e^{-iH_F T}$.

The first Brillouin zone $-\omega \leq E_n \leq \omega$ in quasi-energy contains all of the information that we are interested in, and $U(T)$ becomes $U(\mathbf{k}, T)$, with \mathbf{k} being crystal momentum. More generally, the non-degenerate Floquet-Bloch time-evolution operator at t is

$$U(\mathbf{k}, t) = \sum_{n=1}^N |\epsilon_n(\mathbf{k}, t)\rangle \langle \epsilon_n(\mathbf{k}, t)| e^{-i\phi_n(\mathbf{k}, t)} \quad (5)$$

with the n -th non-degenerate eigenstate $|\epsilon_n(\mathbf{k}, t)\rangle$ of $U(\mathbf{k}, t)$. $\phi_n(\mathbf{k}, t)$ is the pivot of quasi-energy winding. In the mean time, we derive the Floquet Hamiltonian matrix as

$$H_{\alpha, \alpha'}^{l, l'}(\mathbf{k}) = l\omega \delta_{\alpha, \alpha'} \delta_{l, l'} + \frac{1}{T} \int_0^T dt e^{-i(l-l')\omega t} H_{\alpha, \alpha'}(\mathbf{k}, t), \quad (6)$$

where l and l' are the sector indices of quasi-energy, α and α' are the dummy indices of eigenbasis that depend on system size L . The extended Hilbert space of effective Hamiltonian is $(L \times S)^2$ (sector number S). The block diagonal of $H_{\alpha, \alpha'}^{l, l'}$ is dominated by static Hamiltonian by adding $l\omega$. Other block off-diagonal elements of $H_{\alpha, \alpha'}^{l, l'}$ are the driving contribution.

First, we consider how Floquet Weyl semimetals, as shown in Fig. 2, can be generated when periodic driving is turned on. In more details, static Hamiltonian is chosen to be topologically trivial with the parameters of $m = 7t_0$ and $t_s = t_0 = 1$. The band structure centered at quasi-energy 0 is shown in the left panel of Fig. 2. Then, the periodic driving is turned on to the strength of $\Delta_0 = 1.5$. We can numerically solve the Floquet spectrum of Hamiltonian (1) for a cylindrical geometry with the periodic boundary conditions in the z -direction and open boundary conditions in the y -direction. By examining the band centered at quasi-energy 0.5, we see the appearance of the edge states, which suggests the existence of WPs. These Floquet Weyl semimetals can be explained in terms of the effective $m_{\text{eff}} = m - \omega/2$. Note that the static Hamiltonian (1) is only topologically nontrivial in the parameter regime $(2t_0 < m < 6t_0)$. The initial value of $m = 7t_0$ is out of the topological parameter regime. However, the effective $m_{\text{eff}} = m - \omega/2 = 2.5t_0$ is reduced by periodic driving so that the resulting effective Hamiltonian becomes topologically nontrivial.

Next, we show how anomalous Floquet Weyl semimetals can be generated. Initially, static Hamiltonian is chosen to be topologically nontrivial with two Weyl points under the parameters of $m = 4t_0$ and $t_s = t_0 = 1$ [as shown in Fig. 1(d)] or topological trivial without Weyl points [Fig. 1(c)]. Whether Weyl points in the band structure exist depends on the change in the value of $C(k_z)$, i.e., the Chern number of all bands below the gap. Following Ref. [4], we can calculate $C(k_z)$ for the chosen gap. Then, the integer change in the Chern number indicates that the Weyl point can be detected with changing k_z . Indeed, as shown below, the right panel of Fig. 2 demonstrates the existence of anomalous Floquet Weyl semimetals.

Now, we provide a deeper understanding from the point of view of the Chern number to show how the phenomenology discussed in Eq. (4) can arise in the microscopic lattice model without relying on adiabatic projections. As pointed out in Ref. [5], the key observa-

tion is that a straightforward way to calculate the Chern numbers of bands for truncated Floquet Hamiltonian actually exists. Essentially, one can interpret truncated Floquet Hamiltonian as the static Hamiltonian of some new N -band system. With a change in the Chern number, we can demonstrate the position and number of the Weyl points. We use Fig. 3(c1) and (c2) as examples to explain the main points. When $m = 8.0t_0$, no Weyl points in static Hamiltonian [Fig. 1(c)] exist. Remarkably, with periodical driving, we see that in Fig. 3(c1), four new Weyl points show up at $(\pi, 0, k_z \approx \pm 0.67\pi)$ and $(0, \pi, k_z \approx \pm 0.67\pi)$. The jump in the Chern number is two, which shows that two Weyl points appear simultaneously by tuning k_z . For $m = 4.0t_0$, the Weyl points in Fig. 3(c2) at $(0, 0, k_z \approx \pm 0.48\pi)$ and $(\pi, \pi, k_z \approx \pm 0.67\pi)$ are responsible for the jumps in the change in the Chern number. The number is doubled compared to that of the static case. For the former, the mechanism is described in Eq. (2), where periodic driving can effectively change m . For the latter, the periodic driving can dramatically change the band structure to create new Weyl points. Therefore, periodic driving offers a novel way to manipulate Weyl points in the system that we explored. It can be a generic way to change the topological properties of quantum systems.

Experimental realization and summary—Owing to the recent progress in the simulation of topological quantum matter with ultracold gases in optical lattices, Hamiltonian (1) can be simulated experimentally with ultracold fermionic atoms in 3D optical lattices. The spin degree of freedom can be encoded by two atomic internal states or sublattices. Then, the required spin-flipping hopping can be realized by synthetic spin-orbit coupling or magnetic field in the xy plane; finally, the σ_z term can be generated by similar external laser-atom dressing. The components that allow to realize Hamiltonian (1) in optical lattices are well within the experimental reach with an extension. In a broader context, the tunable Weyl-semimetal bands can be simulated using superconducting quantum circuits. By driving the superconducting quantum circuits with microwave fields, Ref. [30] mapped the momentum space of a lattice to the parameter space, which realized the Hamiltonian of the Weyl semimetal. At the same time, the topological winding numbers were further determined from the Berry curvature measurement. In summary, we hope that the predicted Floquet and anomalous Floquet Weyl semimetals in this work can be observed in the abovementioned physical systems.

We thank Ying Hu, Chao Gao, Wei Yi, and Biao Wu for inspiring discussion. This work is supported by the key projects of the Natural Science Foundation of China (Grant Nos. 11835011 and 11774316). T. Q. is supported by the start-up fund (Grant No. S020118002/069) from Anhui University.

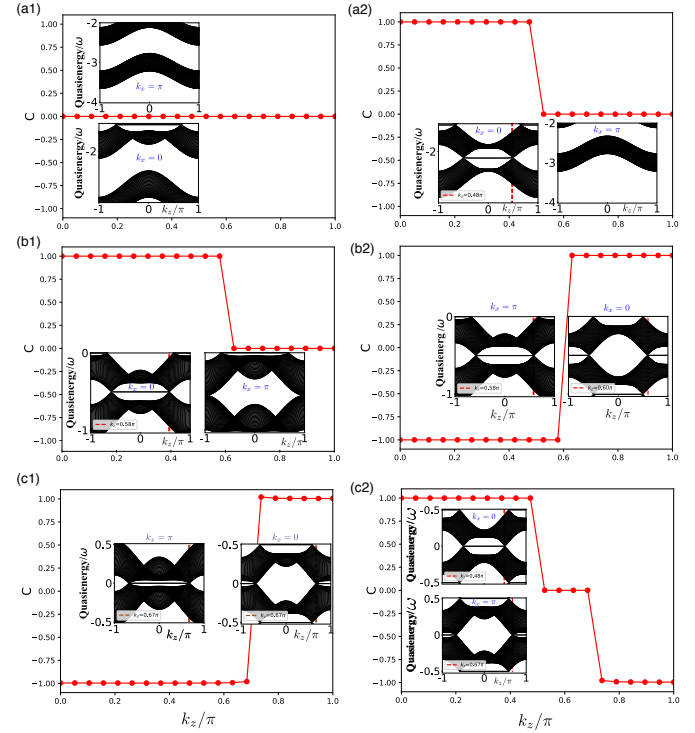


FIG. 3. Chern number for the lowest $LS/2 - 2$, $LS/2 - 1$ and $LS/2$ bands, and the corresponding quasi-energy spectrum. $S = 5$ in our calculation. A change in the Chern number reveals the position of the number of Weyl points. The parameters in left and right panels are the same as the corresponding ones in Fig. 2.

* gaoxl@zjnu.edu.cn

† zhxliang@zjnu.edu.cn

- [1] Thomas Schuster, Snir Gazit, Joel E. Moore, and Norman Y. Yao, “Floquet hopf insulators,” *Phys. Rev. Lett.* **123**, 266803 (2019).
- [2] Takuya Kitagawa, Erez Berg, Mark Rudner, and Eugene Demler, “Topological characterization of periodically driven quantum systems,” *Phys. Rev. B* **82**, 235114 (2010).
- [3] Liang Jiang, Takuya Kitagawa, Jason Alicea, A. R. Akhmerov, David Pekker, Gil Refael, J. Ignacio Cirac, Eugene Demler, Mikhail D. Lukin, and Peter Zoller, “Majorana fermions in equilibrium and in driven cold-atom quantum wires,” *Phys. Rev. Lett.* **106**, 220402 (2011).
- [4] Netanel H. Lindner, Gil Refael, and Victor Galitski, “Floquet topological insulator in semiconductor quantum wells,” *Nat. Phys.* **7**, 490 (2011).
- [5] Mark S. Rudner, Netanel H. Lindner, Erez Berg, and Michael Levin, “Anomalous edge states and the bulk-edge correspondence for periodically driven two-dimensional systems,” *Phys. Rev. X* **3**, 031005 (2013).
- [6] Ying Hu, Peter Zoller, and Jan Carl Budich, “Dynamical buildup of a quantized hall response from nontopological states,” *Phys. Rev. Lett.* **117**, 126803 (2016).

[7] Jan Carl Budich, Ying Hu, and Peter Zoller, “Helical floquet channels in 1d lattices,” *Phys. Rev. Lett.* **118**, 105302 (2017).

[8] Frederik Nathan, Mark S. Rudner, Netanel H. Lindner, Erez Berg, and Gil Refael, “Quantized magnetization density in periodically driven systems,” *Phys. Rev. Lett.* **119**, 186801 (2017).

[9] Ivar Martin, Gil Refael, and Bertrand Halperin, “Topological frequency conversion in strongly driven quantum systems,” *Phys. Rev. X* **7**, 041008 (2017).

[10] Shunyu Yao, Zhongbo Yan, and Zhong Wang, “Topological invariants of floquet systems: General formulation, special properties, and floquet topological defects,” *Phys. Rev. B* **96**, 195303 (2017).

[11] F. Nur Ünal, André Eckardt, and Robert-Jan Slager, “Hopf characterization of two-dimensional floquet topological insulators,” *Phys. Rev. Research* **1**, 022003 (2019).

[12] Martin Rodriguez-Vega, Abhishek Kumar, and Babak Seradjeh, “Higher-order floquet topological phases with corner and bulk bound states,” *Phys. Rev. B* **100**, 085138 (2019).

[13] Yang Peng and Gil Refael, “Floquet second-order topological insulators from nonsymmorphic space-time symmetries,” *Phys. Rev. Lett.* **123**, 016806 (2019).

[14] Haiping Hu, Biao Huang, Erhai Zhao, and W. Vincent Liu, “Dynamical singularities of floquet higher-order topological insulators,” *Phys. Rev. Lett.* **124**, 057001 (2020).

[15] Biao Huang and W. Vincent Liu, “Higher-order floquet topological insulators with anomalous corner states,” (2018), arXiv:1811.00555 [cond-mat.str-el].

[16] P. M. Perez-Piskunow, L. E. F. Foa Torres, and Gonzalo Usaj, “Hierarchy of floquet gaps and edge states for driven honeycomb lattices,” *Phys. Rev. A* **91**, 043625 (2015).

[17] Gonzalo Usaj, P. M. Perez-Piskunow, L. E. F. Foa Torres, and C. A. Balseiro, “Irradiated graphene as a tunable floquet topological insulator,” *Phys. Rev. B* **90**, 115423 (2014).

[18] L. E. F. Foa Torres, P. M. Perez-Piskunow, C. A. Balseiro, and Gonzalo Usaj, “Multiterminal conductance of a floquet topological insulator,” *Phys. Rev. Lett.* **113**, 266801 (2014).

[19] P. M. Perez-Piskunow, Gonzalo Usaj, C. A. Balseiro, and L. E. F. Foa Torres, “Floquet chiral edge states in graphene,” *Phys. Rev. B* **89**, 121401 (2014).

[20] Wenchao Hu, Jason C. Pillay, Kan Wu, Michael Pasek, Perry Ping Shum, and Y. D. Chong, “Measurement of a topological edge invariant in a microwave network,” *Phys. Rev. X* **5**, 011012 (2015).

[21] B. Q. Lv, H. M. Weng, B. B. Fu, X. P. Wang, H. Miao, J. Ma, P. Richard, X. C. Huang, L. X. Zhao, G. F. Chen, Z. Fang, X. Dai, T. Qian, and H. Ding, “Experimental discovery of weyl semimetal taas,” *Phys. Rev. X* **5**, 031013 (2015).

[22] Su-Yang Xu, Ilya Belopolski, Nasser Alidoust, Madhab Neupane, Guang Bian, Chenglong Zhang, Raman Sankar, Guoqing Chang, Zhujun Yuan, Chi-Cheng Lee, Shin-Ming Huang, Hao Zheng, Jie Ma, Daniel S. Sanchez, BaoKai Wang, Arun Bansil, Fangcheng Chou, Pavel P. Shibayev, Hsin Lin, Shuang Jia, and M. Zahid Hasan, “Discovery of a weyl fermion semimetal and topological fermi arcs,” *Science* **349**, 613–617 (2015).

[23] Su-Yang Xu, Ilya Belopolski, Daniel S. Sanchez, Madhab Neupane, Guoqing Chang, Koichiro Yaji, Zhujun Yuan, Chenglong Zhang, Kenta Kuroda, Guang Bian, Cheng Guo, Hong Lu, Tay-Rong Chang, Nasser Alidoust, Hao Zheng, Chi-Cheng Lee, Shin-Ming Huang, Chuang-Han Hsu, Horng-Tay Jeng, Arun Bansil, Titus Neupert, Fumio Komori, Takeshi Kondo, Shik Shin, Hsin Lin, Shuang Jia, and M. Zahid Hasan, “Spin polarization and texture of the fermi arcs in the weyl fermion semimetal taas,” *Phys. Rev. Lett.* **116**, 096801 (2016).

[24] Xiao-Qi Sun, Shou-Cheng Zhang, and Tomáš Bzdušek, “Conversion rules for weyl points and nodal lines in topological media,” *Phys. Rev. Lett.* **121**, 106402 (2018).

[25] A. A. Zyuzin and A. A. Burkov, “Topological response in weyl semimetals and the chiral anomaly,” *Phys. Rev. B* **86**, 115133 (2012).

[26] Chao-Xing Liu, Peng Ye, and Xiao-Liang Qi, “Chiral gauge field and axial anomaly in a weyl semimetal,” *Phys. Rev. B* **87**, 235306 (2013).

[27] A. A. Burkov, “Chiral anomaly and diffusive magnetotransport in weyl metals,” *Phys. Rev. Lett.* **113**, 247203 (2014).

[28] S. A. Parameswaran, T. Grover, D. A. Abanin, D. A. Pesin, and A. Vishwanath, “Probing the chiral anomaly with nonlocal transport in three-dimensional topological semimetals,” *Phys. Rev. X* **4**, 031035 (2014).

[29] Xiao-Qi Sun, Shou-Cheng Zhang, and Zhong Wang, “Helical spin order from topological dirac and weyl semimetals,” *Phys. Rev. Lett.* **115**, 076802 (2015).

[30] Xinsheng Tan, Y. X. Zhao, Qiang Liu, Guangming Xue, Hai-Feng Yu, Z. D. Wang, and Yang Yu, “Simulation and manipulation of tunable weyl-semimetal bands using superconducting quantum circuits,” *Phys. Rev. Lett.* **122**, 010501 (2019).

[31] M. M. Vazifeh and M. Franz, “Electromagnetic response of weyl semimetals,” *Phys. Rev. Lett.* **111**, 027201 (2013).

[32] P. Baireuther, J. A. Hutasoit, J. Tworzydło, and C. W. J. Beenakker, “Scattering theory of the chiral magnetic effect in a weyl semimetal: interplay of bulk weyl cones and surface fermi arcs,” *New Journal of Physics* **18**, 045009 (2016).

[33] Sho Higashikawa, Masaya Nakagawa, and Masahito Ueda, “Floquet chiral magnetic effect,” *Phys. Rev. Lett.* **123**, 066403 (2019).

[34] Valerio Peri and Sebastian D. Huber, “Anomalous fermi arcs in a periodically driven weyl system,” (2018), arXiv:1812.06994 [cond-mat.mes-hall].

[35] Zhongbo Yan and Zhong Wang, “Tunable weyl points in periodically driven nodal line semimetals,” *Phys. Rev. Lett.* **117**, 087402 (2016).

[36] N. P. Armitage, E. J. Mele, and Ashvin Vishwanath, “Weyl and dirac semimetals in three-dimensional solids,” *Rev. Mod. Phys.* **90**, 015001 (2018).